Volume 4 Issue 2 (September 2024)
DOI 10.24191/jaeds.v4i2.86
eISSN 2805-5756

Journal of Applied Engineering Design & Simulation

Numerical Analysis on the Effect of Building Spacing and Podium on the Flow Structure Over High Rise Residential Buildings

A. A. Rahman[1], M.F. Mohamad[1,2,*] A. Jaffar[3], A. A. Razak[1] and N. Ikegaya[4]
[1]Wind Engineering & Building Physics Center (WEBPC), School of Mechanical Engineering, Universiti Teknologi MARA, Shah Alam 40450 Selangor, Malaysia.
[2]Smart Manufacturing Research Institute (SMRI), Universiti Teknologi MARA, Shah Alam 40450 Selangor, Malaysia.
[3]Malaysia France Institute, Universiti Kuala Lumpur, Bandar Baru Bangi 43650 Selangor, Malaysia.
[4]Faculty of Engineering Sciences, Kyushu University, Japan
[*]corresponding author: faizal3744@uitm.edu.my

ABSTRACT

Urban environments with high-rise buildings often experience intensified wind speeds at the pedestrian level, which can compromise comfort and safety. The growing demand for urban housing has led to the proliferation of such buildings, but the impact of building geometry and configuration on local wind conditions remains underexplored, particularly concerning the presence of podium structures. This study addresses the critical issue of pedestrian-level wind (PLW) by investigating how the spacing between buildings and the inclusion of podiums affect wind dynamics. Using computational fluid dynamics (CFD) simulations, the study models wind flow around two high-rise residential buildings arranged back-to-back under different spacing configurations (0.16H, 0.31H, and 0.63H) with and without podiums. The primary objective is to assess wind speed ratios and vortex formations to identify optimal design configurations for enhancing pedestrian comfort and safety. The results show that building spacing of 0.31H without podiums yields the lowest wind speed ratio at the pedestrian level, enhancing safety. The introduction of a podium significantly alters wind flow patterns, particularly by increasing downwash flow and generating larger vortices above the podium level, which can exacerbate wind speeds at higher elevations. These findings underscore the importance of careful urban design considerations, particularly regarding building spacing and podium integration, to mitigate adverse wind effects. The study provides actionable insights for architects and urban planners to create wind-sensitive designs that improve the quality of life in densely built environments.

Keywords: wind comfort; urban flow; RANS; podium; pedestrian safety

Nomenclature (Greek symbols towards the end)

u	streamwise velocity in the x-direction (m/s)
v	lateral velocity in the y-direction (m/s)
w	vertical velocity in the z-direction (m/s)
U	velocity magnitude (m/s)
u_{ref}	reference approaching velocity at building height (m/s)
k	turbulent kinetic energy (m^2/s^2)
ε	turbulence dissipation rate (m^2/s^3)
H	building height (m)

Abbreviations

CFD	computational fluid dynamics
WTE	wind tunnel experiment
3D	three dimensional
RANS	Reynolds-Averaged Navier-Stokes

Received on 02.09.2024
Accepted on 20.09.2024
Published on 27.09.2024

1.0 INTRODUCTION

The rapid urbanization of cities around the world has resulted in the widespread construction of high-rise residential buildings to address the growing demand for housing. These structures, while essential for addressing housing shortages, significantly impact the microclimate of their immediate surroundings, particularly in terms of wind conditions at the pedestrian level. Pedestrian-level wind (PLW) is a crucial consideration in urban planning and design, as it directly influences the comfort, safety, and usability of outdoor spaces in dense urban environments. PLW speeds in the built environment are significantly influenced by the presence of buildings, especially high-rise structures, and their surrounding configurations [1].

Wind conditions at the pedestrian level can lead to various issues, including discomfort and safety hazards, especially in areas where wind speeds are intensified by the presence of tall buildings [2]. High wind speeds at pedestrian level in high building can reduce the usability of public spaces and create potentially hazardous conditions for pedestrians, especially for vulnerable groups [3]. Addressing and mitigating these wind effects is therefore essential for creating liveable urban environments.

The configuration and orientation of high-rise buildings are crucial factors that determine local wind patterns. When two high-rise buildings are positioned opposite each other, the resulting wind flow can become complex and often lead to accelerated wind speeds at pedestrian levels [4]. To address these adverse wind effects, architects and urban planners have explored various design strategies. One such strategy involves the use of podium structures at the base of high-rise buildings. These podiums act as windbreaks, modifying wind flow patterns and reducing the impact of high wind speeds on pedestrians [5]. Recent studies have shown that podium structures can significantly improve wind conditions at pedestrian levels, enhancing both comfort and safety in urban environments [6], [7]. In Malaysia, the podium serves not only as a shopping center and parking lot, but also as a recreational platform with a swimming pool and an integrated garden for the use of residents. However, the designated common area above the podium receives less attention than the lower portion where the majority of studies are undertaken on the assessment of the wind environment [4], [6], [8], [9].

Wind tunnel experiments (WTE) and computational fluid dynamics (CFD) simulations are commonly used to study these effects, providing critical insights into how different building configurations influence wind behaviour. These methods have proven to be effective tools for predicting and analysing pedestrian-level wind conditions, making them indispensable for developing urban design guidelines that prioritize liveability.

1.1 Research significance

This research aims to contribute to the development of more effective urban design strategies that enhance pedestrian comfort and safety. By examining the wind environment around high-rise buildings with and without podiums, this study intends to provide empirical data that can guide better building design practices. The novelty of this research is emphasized by its specific focus on comparing wind environments in the presence and absence of podium structures, a topic that has been relatively underexplored in existing literature.

Previous research has largely concentrated on how building height and orientation affect pedestrian-level wind conditions [9], [10]. However, there is a noticeable gap in the literature concerning the impact of podium structures on these wind patterns. Existing studies suggest that podiums can effectively reduce wind speeds at ground level, but the extent and reliability of this impact require further investigation. This research seeks to fill this gap by systematically comparing wind environments with and without podiums, utilizing CFD in contrast to wind tunnel experiments for the prediction and assessment of pedestrian wind environments. This methodology is expected to provide robust evidence on the effectiveness of podiums in mitigating adverse wind effects at pedestrian levels.

1.2 Problem statement

The central problem addressed by this research is the lack of comprehensive data on the role of podium structures in managing pedestrian-level wind conditions. Although podiums are commonly used in architectural designs, their specific impact on wind patterns at ground level has not been extensively studied. This research aims to address this gap by comparing the wind environment around high-rise buildings with and without podiums.

The objectives of this study are twofold: (1) to investigate the wind environment around high-rise buildings with and without podium structures; and (2) to evaluate predestrian level wind (PLW) conditions within the common area designated on the top of the podium. The scope of the research is limited to CFD simulation focused on high-rise residential buildings in urban environments.

This research is expected to have significant implications for urban design and planning, particularly in improving the liveability of high-density urban areas. By providing empirical data on the effectiveness of podiums in managing pedestrian-level wind conditions, this study aims to inform the development of more effective urban design guidelines. The findings could lead to a direct impact on the design of high-rise buildings, contributing to enhanced pedestrian comfort and safety.

In summary, this study addresses a critical gap in the literature by systematically comparing the wind environment around high-rise buildings with and without podium structures. The study's findings are expected to offer valuable insights into the role of podiums in mitigating adverse wind effects at pedestrian levels, thereby contributing to the creation of more liveable urban spaces. The novelty of this research lies in its focused examination of podium structures, an area that has not been thoroughly explored in previous studies. The use of wind tunnel experiments is expected to provide strong evidence of the effectiveness of podiums in enhancing pedestrian comfort and safety in urban settings.

2.0 METHODOLOGY

2.1 Building geometry and computational domain

The simulations are performed on two separate buildings positioned in a back-to-back arrangement, parallel with the direction of the incoming flow, as illustrated in Fig. 1. Each building has a depth of 0.5*H*, a width of 0.5*H*, and a height of *H*, resulting in a building configuration with a ratio of 1:1:2. The buildings are designed to scale, with dimensions of 40 m (depth) x 40 m (width) x 80 m (height), using a ratio of 1:400. The simulations are conducted on two different configurations, one without a podium and that with a podium. The distance between two buildings is adjusted to be 0.16*H*, 0.31*H*, and 0.63*H*. However, for the podium, only the depth is modified to be 1.66*H*, 1.81*H*, and 2.13*H* aligned with the distance of the two buildings. The height and width remain fixed at 0.25*H* and *H*, respectively. Hence, the simulations are categorized into six different scenarios, specifically Case1, Case2, Case3, Case4, Case5, and Case6, as illustrated in Fig.1(a)-(f).

The buildings are positioned within the simulation domain, as depicted in Fig. 2, following the recommended guidelines for best arrangement [11], [12]. The blockage ratio resulting from the established domain is approximately 1%. The upwind boundary is denoted by the inlet, which is located 3*H* from the windward façade. Furthermore, the outlet boundary is positioned 15*H* downstream from the leeward façade of the rear building, providing adequate distance to replicate the reverse flow that occurs behind the model. The vertical extent of the domain is defined as 6*H*, while the front and back boundaries are spaced apart by a distance equal to 11 times the height of the building.

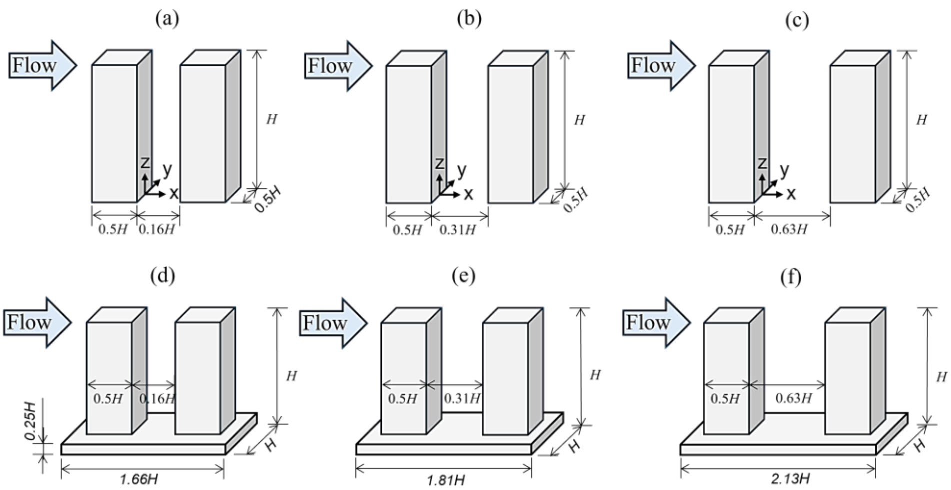

Figure 1. Buildings arrangements under conditions of without and with podium (a) Case1 (b) Case 2 (c) Case 3 (d) Case4 (e) Case5 and (f) Case6 (*Please note that the diagram is not drawn to scale in order to provide a clearer visual representation*)

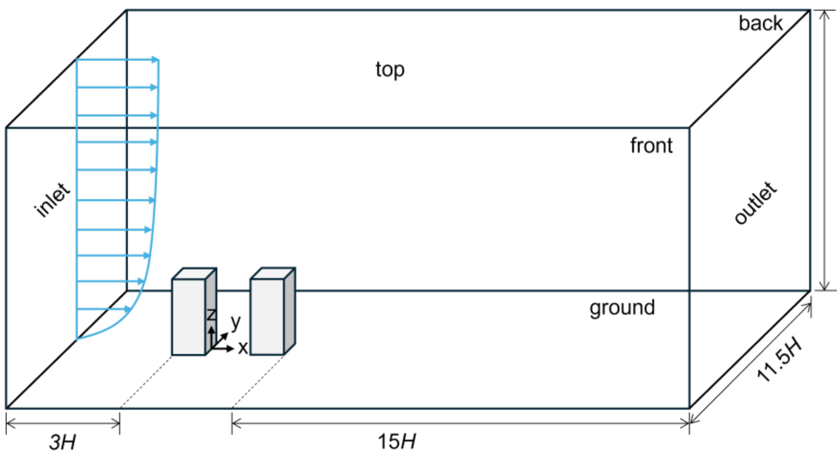

Figure 2. Schematic representation of simulation domain and arrangement of the buildings

2.2 Boundary conditions and solver settings

At the inlet boundary, wind velocity profile is defined corresponding to the power law of index $\alpha = 0.25$ as shown in Eq. (1).

$$\frac{u(z)}{u_{ref}} = \left(\frac{z}{H}\right)^{\alpha} \tag{1}$$

The reference velocity at the building height, denoted as u_{ref} is 4.2 m/s. The height coordinate is represented by z. The building Reynolds number ($Re = u_{ref}H/\nu$, where ν is the kinematic viscosity taken as 1.5×10^{-5} m^2/s) is 56,000. The profiles of turbulent kinetic energy k [13] and turbulent dissipation rate ε [11] are approximated by the following expressions:

$$\frac{k(z)}{u_{ref}^2} = 0.033\, exp\left(-0.32\left(\frac{z}{H}\right)\right) \tag{2}$$

$$\varepsilon(z) = C_\mu^{1/2} k(z) \frac{u_{ref}}{H} \alpha \left(\frac{z}{H}\right)^{(\alpha-1)} \tag{3}$$

where C_μ is a model constant equal to 0.09.

At the outflow boundary, zero static pressure is applied. For the top boundary, slip boundary conditions is adopted while zero normal velocity and zero normal gradient for all variables are defined at the lateral sides of the domain. Standard wall functions are applied to the building and ground surfaces.

2.3 Solver settings

The open-source software Open Field Operation and Manipulation (OpenFOAM-v2212) is used to conduct a series of 3D Reynolds-Averaged Navier-Stokes (RANS) simulations under steady state and isothermal conditions. The renormalization group k-ε (RNG) closure model is chosen because it outperforms other closure models such as the standard k-ε (STD) and realizable k-ε (RLZ) models [14]. The Semi-implicit Method for Pressure-linked Equation (SIMPLE) algorithm is used to solve the pressure velocity coupling. In addition, the momentum equation utilizes an explicit second-order upwind scheme [15] for the convective terms. Meanwhile, the convective terms in the transport equations of turbulent kinetic energy and turbulent dissipation rate are discretized by a total variation diminishing (TVD) method [16]. The pressure residual is set to 10^{-5}, while the convergence monitoring residuals for momentum, turbulent kinetic energy, and turbulent dissipation rate are set to 10^{-6}.

2.4 Validation

As illustrated in Fig. 3(a), a validation study was carried out in compliance with the wind tunnel experiment (WTE) conducted at Tokyo Polytechnic University, Japan, under single isolated 1:1:2 building settings [17] before the primary simulations. Fig. 3(b) illustrates the domain that is generated according to the recommendations for simulating atmospheric boundary layer conditions, as described in references [11] and [12]. Furthermore, Fig. 3(c) depicts the particular points of measurement that are being compared between the WTE results and the simulation data. The light blue plane is positioned on the *x-z* plane at *y/H*=0.0. The light green plane is positioned horizontally on the *x-y* plane at *z/H*=0.0625, which corresponds to the height of a pedestrian.

Fig. 4 depicts the normalized velocity profiles for *u*, *v*, and *w* components measured over the vertical plane at *y/H*=0 and the horizontal plane at *z/H*=0.0625. CFD simulations demonstrate an excellent match with the reference data, especially in the areas of interest such as the windward and leeward sides of the structures. The observed wind speed ratios and flow structures around the buildings exhibit a strong agreement with the experimental data, suggesting that the model effectively represents the fundamental aerodynamic characteristics of the investigated building designs. Overall, the trends are uniform, with some slight deviations in specific areas especially for streamwise velocity far downstream of the building at *x/H* = 0.75 and 1.25. This occurrence can be attributed to the nature of the RANS model, which tends to overestimate the length of reattachment, thereby leading to the development of reverse flow opposed to the observed experimental data. The observed deviations are generally modest and have minimal effect on the research's overall findings considering the areas under investigation do not extend beyond the previously indicated distances. The validation of the CFD model against the reference data significantly increases the confidence in the simulation results reported in the paper. The confirmation of the model's ability to precisely forecast wind flow patterns around structures establishes the relevance and reliability of the findings for real-world applications in urban planning and architecture.

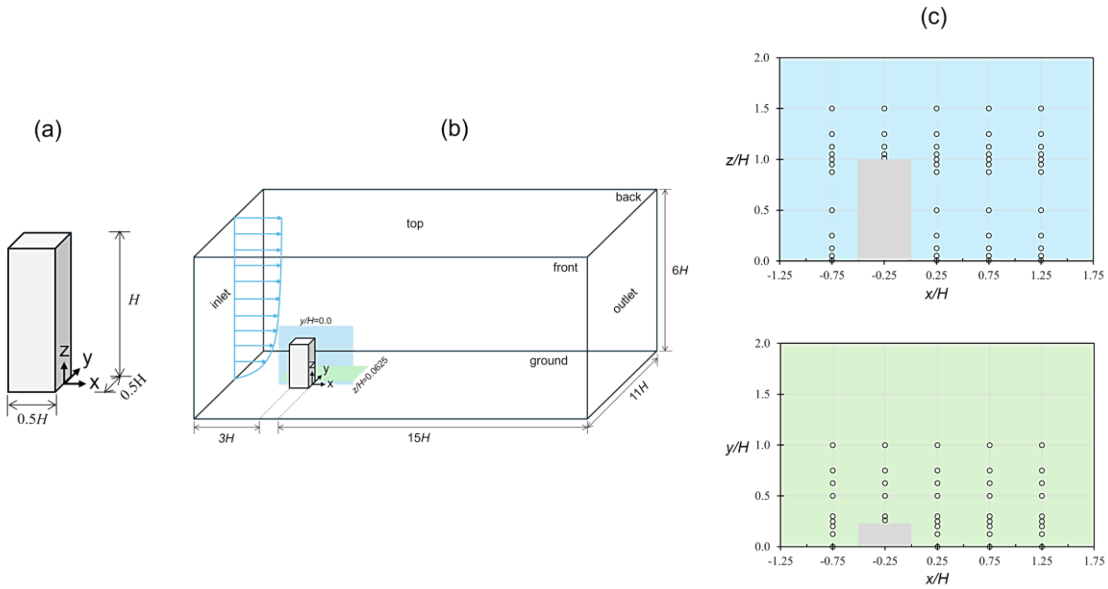

Figure 3. Details of the (a) building dimensions (b) simulation domain and (c) measurement points adopted in the validation study.

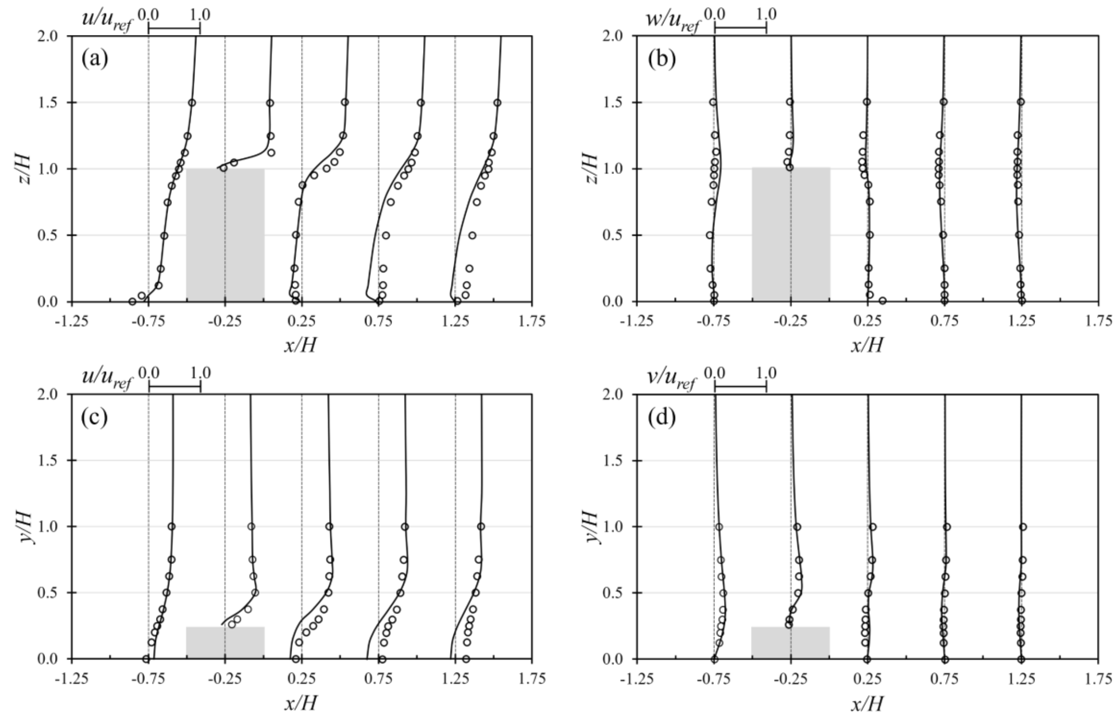

Figure 4. Comparison between current simulation (*solid line*) and WTE (*empty circle*) results for two different planes (a)(b) *x-z* plane at *y/H*=0.0 and (c)(d) *x-y* plane at *z/H*=0.0625.

2.5 Grid sensitivity study

Grid sensitivity analysis is performed on three different mesh distributions: coarse (Fig. 5(a)), medium (Fig. 5(b)), and fine (Fig. 5(c)). Each distribution has a total of 0.6 million, 1.5 million, and 3.1 million grids, respectively. The velocity profiles of normalized *u*, *v*, and *w* at six measurement locations on the *x-z* plane at y/H=0 (Fig. 5(d) and (e)) and *x-y* plane at z/H=0.0625 (Fig. 5(f) and (g)) are being compared. The analysis revealed that the wind speed ratios and flow patterns exhibited a high degree of stability when the grid undergone refinement from a coarse to a medium resolution. This observation suggests that the medium grid adequately captured the essential characteristics of the wind flow without compromising its accuracy. No significant changes were observed in the findings when the grid was further refined to a fine resolution, indicating that the medium grid achieved a satisfactory equilibrium between accuracy and computational efficiency. The minimal disparities between the medium and fine grids suggest that the medium grid is sufficient for the simulations, therefore assuring that the observed outcomes are not influenced by the resolution of the grid. The final simulations in the work were conducted using the medium grid resolution, as determined by the grid sensitivity analysis. The justification for this decision is supported by the limited difference in outcomes between the medium and fine grids, suggesting that additional refinement would not greatly enhance precision but would raise the computing cost. The analysis validates that the chosen grid resolution is suitable for precisely capturing the wind flow characteristics around the buildings, therefore assuring the dependability of the study's findings.

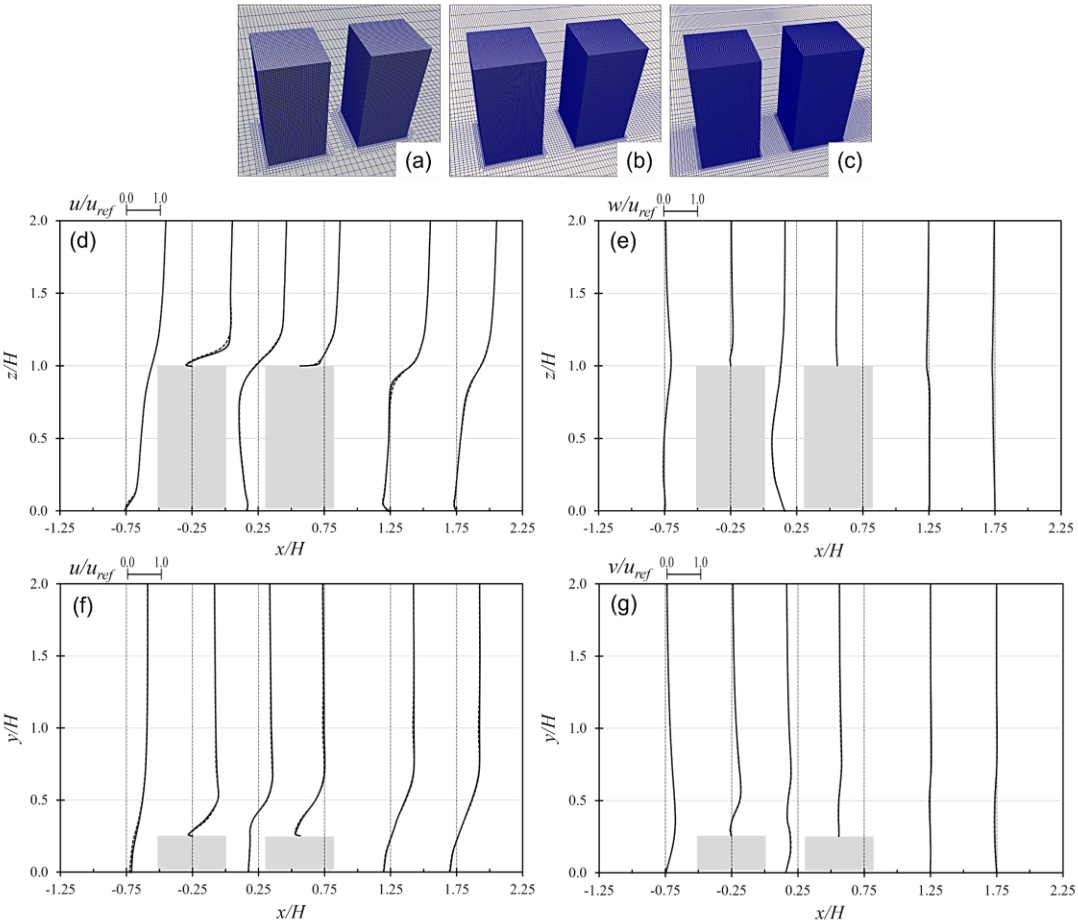

Figure 5. Grid distributions over buildings and vicinity area with (a) coarse (b) medium and (c) fine meshes, respectively. Velocities comparison for (d)(e) vertical plane at *y/H*=0.0 and (f)(g) horizontal plane at *z/H*=0.0625. Lines are presented through *dashed-line*; coarse mesh, *solid line*; medium mesh and *dotted-line*; fine mesh.

3.0 RESULTS AND DISCUSSION

The results are analysed in the sample planes both vertically and horizontally, depending on whether podium is present or not. On the vertical plane, the position remains constant at *y/H*= 0, regardless of the presence of the podium. However, the position on the horizontal plane is adjusted to accurately represent the pedestrian area that surrounds the entire building. In the scenarios where there is no podium (Case1, Case2, and Case3), the location is at *z/H*= 0.0625. However, for the cases with a podium (Case4, Case5, and Case6), the evaluations are carried out at *z/H*= 0.3125, which represents the common area above the podium.

Fig. 6 illustrates the comparison of dimensionless mean wind speed and superimposed velocity vector at two particular positions (*y/H*= 0.0 and *z/H*= 0.0625) for three different scenarios (Case1, Case2, and Case3) under the condition of no podium. As seen in Fig. 6(a)~(c), a standing vortex at the pedestrian level produced by the downward flow is observed in front of the upstream building in all cases. A small vortex can be observed between the buildings in the upper left corner of Case1, becoming increasingly apparent as the distance between buildings increases in Case2 and Case3. This is evidence that the shear flow is forced downward by the downstream building corner, allowing for greater penetration of the flow above into the gap between the buildings as the distance increases. In addition, in the horizontal planes depicted in Figure 6(d)~(f), the pattern of the corner streams (indicated by the yellow area) remains unchange, as there is no notable alteration in the maximum value within these areas. The highest mean wind speed (U/u_{ref}) in the corner streams for all cases is 0.92 (Case3), 0.93 (Case2), and 0.94 (Case1). The flow between the buildings in Fig. 6(d) is more perpendicular to the building axis as it escapes the restricted area. As the distance between the buildings increases, the flow structures change and oriented into the right diagonal (see Fig. 6(e)). However, in contrast to the previously mentioned two scenarios, when the penetration of the flow above increases, the pedestrian level wind pattern is significantly altered with the reverse flow becoming more prominent (Fig. 6(f)).

Fig. 7 demonstrates the comparison of dimensionless wind speed and superimposed velocity vector for three cases (Case4, Case5, and Case6) under podium conditions. The evaluations are conducted in the vertical plane at *y/H*= 0.0 and at two separate elevations of horizontal planes at *z/H*= 0.0625 (close to ground level) and *z/H*= 0.3125 (above the podium). In contrast to the situation where there is no podium, there are two standing vortices observed in front of the building. One resides in the lower part of the podium, while the other is at the corner of the podium-building. Indeed, the identical outcomes are observed in all cases involving podiums (Fig. 7(a)~(c)). A similar observation with no podium conditions is shown between the building's areas of separation. At a height of *z/H*=0.0625 (as shown in Figure 6(d)~(f)), a separation flow occurs, leading to a reverse flow at both corners of the podium. The highest value of the mean wind speed in the corner stream, $U/u_{ref} \approx 0.82$, is seen in all cases, which represents a reduction of roughly 13% compared to cases without a podium.

At a height of *z/H* = 0.3125 above the podium (Fig. 7(g)~(i)), the maximum wind speed is greater than at a height of *z/H* = 0.0625 since the approaching flow at this elevation is stronger than near the ground. Nevertheless, the value is comparable to the events where there is no podium at *z/H*= 0.0625. Moreover, a distinct reverse flow is depicted on both sides of the upstream building. This is attributed to a combination of flow detachment at the windward corners and the upstream-direction flow approaching from the gap between buildings. In Case1 and Case2, the flow between the buildings is predominantly horizontal in the lateral direction. This is in contrast to the absence of a podium scenario, where a distinct trend is observed. However, in the case with the greatest distance (Fig. 7(i), Case3), the flow pattern remains identical to the case without a podium, despite the difference in evaluation height.

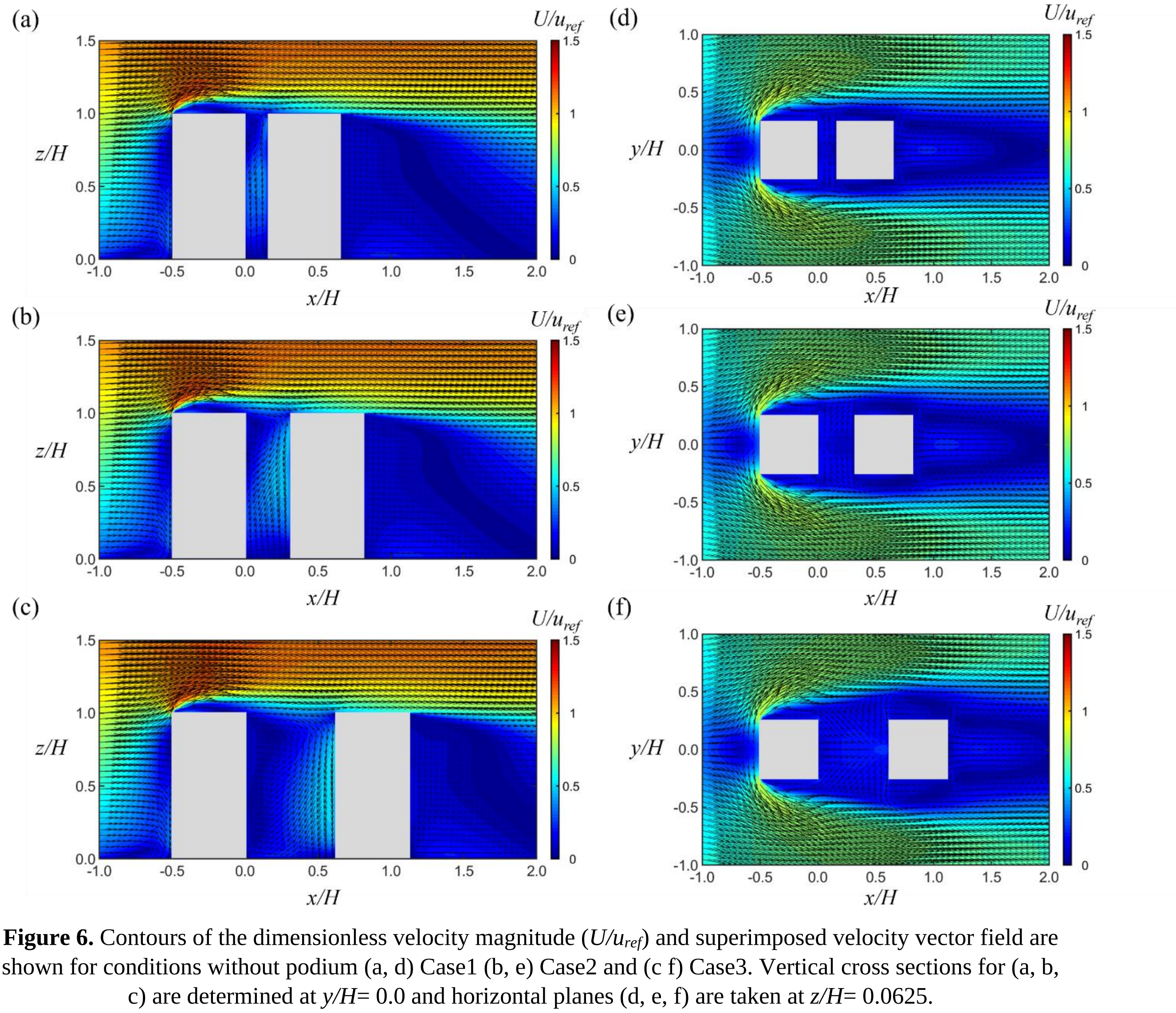

Figure 6. Contours of the dimensionless velocity magnitude (U/u_{ref}) and superimposed velocity vector field are shown for conditions without podium (a, d) Case1 (b, e) Case2 and (c f) Case3. Vertical cross sections for (a, b, c) are determined at *y/H*= 0.0 and horizontal planes (d, e, f) are taken at *z/H*= 0.0625.

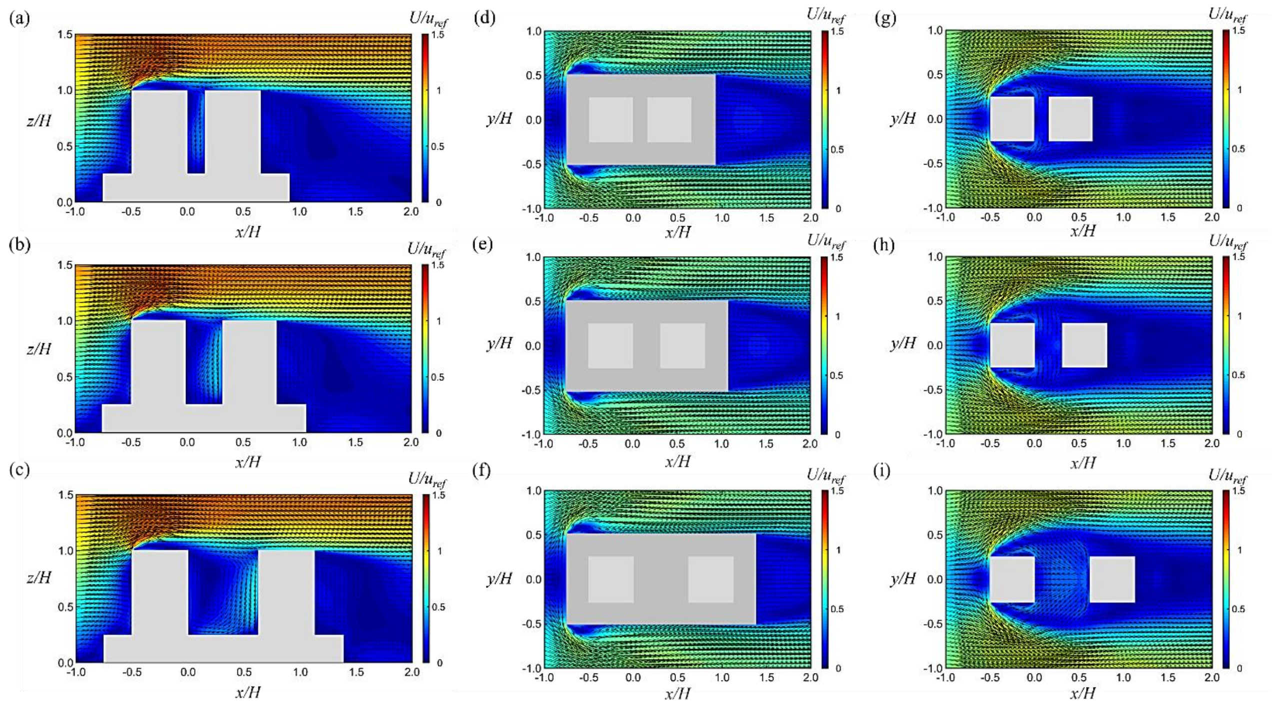

Figure 7. Contours of the dimensionless velocity magnitude (U/u_{ref}) and the velocity vector field are shown for conditions with podium (a, d) Case1 (b, e) Case2 and (c f) Case3. Vertical cross sections for (a, b, c) are determined at *y/H*= 0.0 while horizontal planes (d, e, f) and (g, h, i) are taken at *z/H*= 0.0625 and 0.3125, respectively.

Fig. 8 displays the dimensionless mean wind speed and velocity vector in the *y-z* plane at the central position between the buildings for every case. When there is no podium, the structures exhibit a vertically elongated recirculation region on both sides. In Case1 and Case2, the dominant downwash flow is concentrated in the middle area, but it is more horizontally spread in the y-direction within the width of the buildings in the Case3. In the presence of a podium, increased downwash flow creates larger vortices that are visible on the sides of the structure, as depicted in Figure 8(d)~(f). The flow is dispersed more evenly over the width of the building due to the enforcement of a change in direction by the podium, resulting in a more stronger lateral flow. Furthermore, there are two counter-rotating vortices at the podium height on both sides, which indicate intricate flow interactions with the building structure.

Fig. 9 indicates the mean wind speed ratio along the center axis for both cases with and without a podium. It should be noted that the central position for each case varies depending on the distance between buildings and the elevations corresponding to the podium design. However, in order to better comprehend the overall flow contribution within the gap, a central line is chosen for consistency in evaluating the data. Among the cases without a podium, Case2 has the lowest wind speed ratio within the range of $-0.125 \leq y/H \leq 0.125$, followed by Case1 with an approximate increase of 14%. This is because, in this position, the downward velocity component for Case1 is significantly bigger than Case2, with only slight differences observed for the streamwise and lateral velocity components. A curve with an ellipsoid shape and the highest ratio is plotted in the middle of the building width for the largest building separation (Case3). In the case with podium, a contrast observation for without podium can be confirmed in the Case4 and Case5 as the smallest gap resulting into lowest wind speed ratio within the middle region of the building width. In addition, an identical line trend with Case3 is depicted for the Case6 but with higher wind speed ratio.

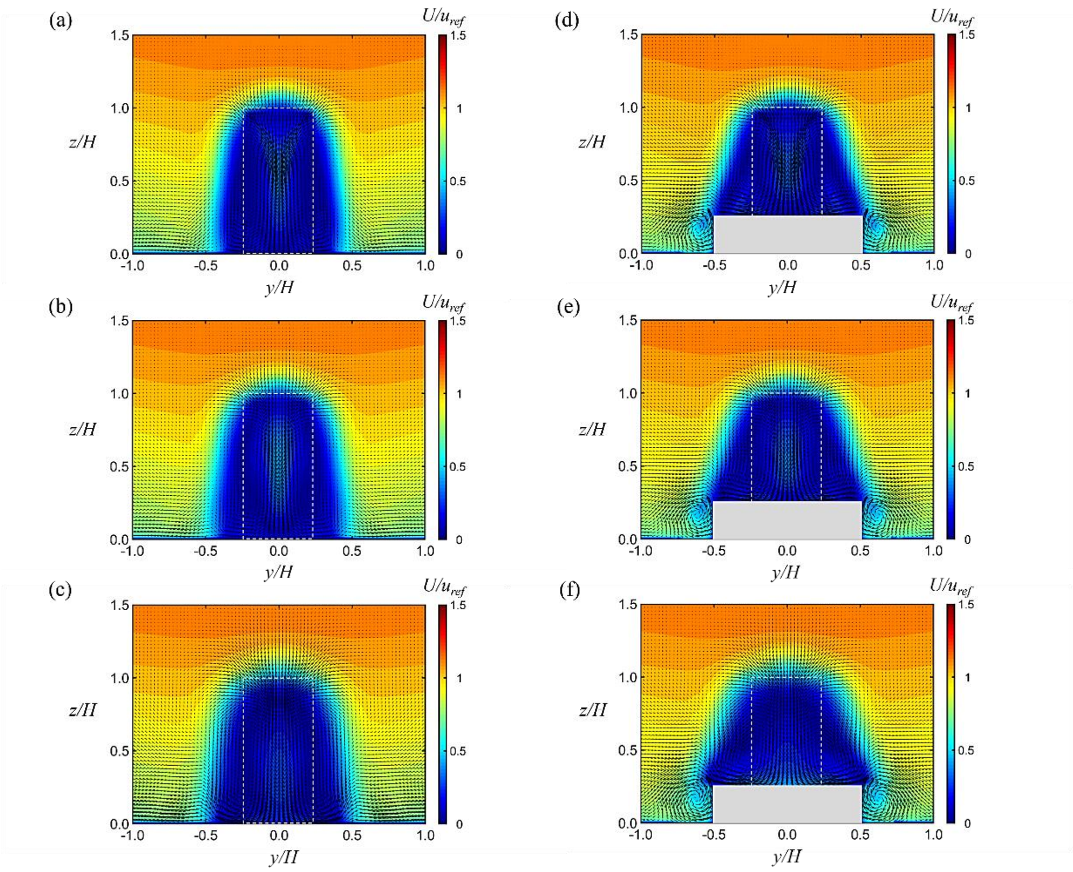

Figure 8. Contours of the dimensionless velocity magnitude (U/u_{ref}) and the velocity vector field determined in *y-z* plane at middle position between buildings for (a) Case1 (b) Case2 (c) Case3 (d) Case4 (e) Case5 and (f) Case6.

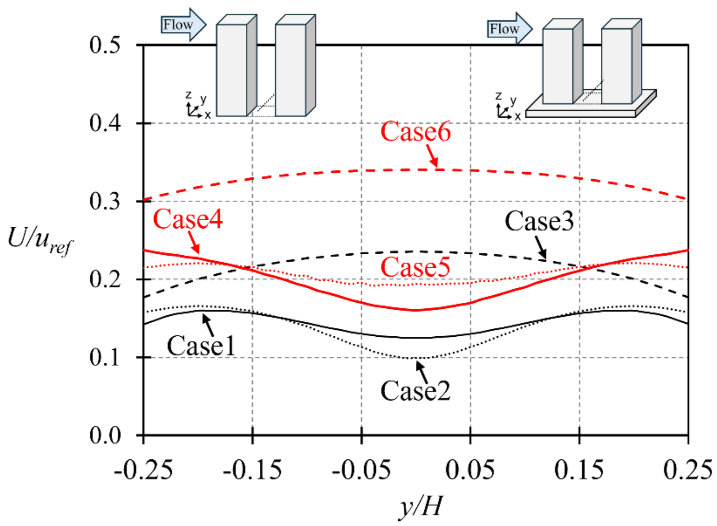

Figure 9. Mean wind speed ratio along the central axis of the passage for all simulated cases. The black lines indicate the measurement lines at a height of z/H= 0.0625 without a podium, whilst the red lines depict the measurement lines at a height of z/H= 0.3125 with a podium.

4.0 CONCLUSION

A series of computational fluid dynamics (CFD) simulations are performed on two buildings arranged in a back-to-back configuration, aligned with the incoming flow. The aim is to investigate the effects of the spacing between the buildings on the flow within and around the area, as well as the wind conditions at pedestrian level. Buildings are categorized into three distances: 0.16H, 0.31H, and 0.63H, both with and without a podium. The simulations are conducted using steady RANS with RNG k-ε model as the closure model. The main conclusions of this investigation are outlined below, based on the data obtained.

- Compared to the building passage, Case 2 without a podium has the lowest wind speed ratio at the pedestrian level. In contrast, Case 4 with a podium exhibits the lowest wind speed ratio within the building's mid-width at the pedestrian height within the common area. Both situations are expected to produce favorable wind conditions while ensuring sufficient ventilation to prevent stagnant air, which can otherwise compromise the air quality.
- The presence of a podium significantly alters the flow structure around the building, resulting in the development of two counter-rotating vortices on both sides. This phenomenon is not observed when there is no podium.

Additional investigations are necessary to clarify the impact of podiums on the wind conditions at pedestrian level. The current study is limited to the specific setting mentioned above, and future recommendations have been provided.

- The study focuses on wind flows that come from only one direction, which may restrict the relevance of the findings to contexts where wind directions vary considerably. Future research should incorporate various wind directions to have a more full understanding of the impact of wind in intricate urban settings.
- The study uses simplified building geometry and spacing, which may not comprehensively capture the complexity of real-world urban layouts. Further investigation of complex architectural forms and arrangements may have diverse outcomes, and future research could investigate these variances to enhance knowledge in the field of urban planning.
- This study did not take into account other environmental elements, such as heat effects, surface roughness, and varying building heights. Incorporating these elements into future simulations will improve the accuracy and application of the findings by considering their major impact on wind flow patterns.

Moreover, as the existing wind tunnel data on the flow over high-rise structures are still restricted to the scenario of a single building, the present simulation is inevitably being validated using the same approach, despite our primary focus is on the scenario of two buildings arranged in a back-to-back configuration. In order to gain a deeper understanding of the flow characteristics, it is recommended to conduct an experimental investigation of the flow over two buildings scenario.

ACKNOWLEDGEMENT

The authors express their appreciation to the Wind Engineering & Building Physics Center (WEBPC), School of Mechanical Engineering, College of Engineering, Universiti Teknologi MARA for their provision of a high-performance computer supporting the completion of this work.

REFERENCES

[1] T. van Druenen, T. van Hooff, H. Montazeri, and B. Blocken, "CFD evaluation of building geometry modifications to reduce pedestrian-level wind speed," *Build Environ*, vol. 163, Oct. 2019, doi: 10.1016/j.buildenv.2019.106293.

[2] T. Stathopoulos, "Pedestrian level winds and outdoor human comfort," *Journal of Wind Engineering and Industrial Aerodynamics*, vol. 94, no. 11, pp. 769–780, Nov. 2006, doi: 10.1016/j.jweia.2006.06.011.

[3] B. Blocken, T. Stathopoulos, and J. P. A. J. van Beeck, "Pedestrian-level wind conditions around buildings: Review of wind-tunnel and CFD techniques and their accuracy for wind comfort assessment," *Build Environ*, vol. 100, pp. 50–81, May 01, 2016, Elsevier Ltd. doi: 10.1016/j.buildenv.2016.02.004.

[4] Y. Tominaga and M. Shirzadi, "Wind tunnel measurement of three-dimensional turbulent flow structures around a building group: Impact of high-rise buildings on pedestrian wind environment," *Build Environ*, vol. 206, Dec. 2021, doi: 10.1016/j.buildenv.2021.108389.

[5] T. van Druenen, T. van Hooff, H. Montazeri, and B. Blocken, "CFD evaluation of building geometry modifications to reduce pedestrian-level wind speed," *Build Environ*, vol. 163, Oct. 2019, doi: 10.1016/j.buildenv.2019.106293.

[6] T. Stathopoulos, “Pedestrian level winds and outdoor human comfort,” *Journal of Wind Engineering and Industrial Aerodynamics*, vol. 94, no. 11, pp. 769–780, Nov. 2006, doi: 10.1016/j.jweia.2006.06.011.

[7] B. Blocken, T. Stathopoulos, and J. P. A. J. van Beeck, “Pedestrian-level wind conditions around buildings: Review of wind-tunnel and CFD techniques and their accuracy for wind comfort assessment,” *Build Environ*, vol. 100, pp. 50–81, May 01, 2016, Elsevier Ltd. doi: 10.1016/j.buildenv.2016.02.004.

[8] Y. Tominaga and M. Shirzadi, “Wind tunnel measurement of three-dimensional turbulent flow structures around a building group: Impact of high-rise buildings on pedestrian wind environment,” *Build Environ*, vol. 206, Dec. 2021, doi: 10.1016/j.buildenv.2021.108389.

[9] S. Zhang and X. Xu, “Pedestrian level wind around super-Tall building: Effects of podium,” in *IOP Conference Series: Earth and Environmental Science*, Institute of Physics Publishing, Feb. 2019. doi: 10.1088/1755-1315/218/1/012036.

[10] C. W. Tsang, K. C. S. Kwok, and P. A. Hitchcock, “Wind tunnel study of pedestrian level wind environment around tall buildings: Effects of building dimensions, separation and podium,” *Build Environ*, vol. 49, no. 1, pp. 167–181, 2012, doi: 10.1016/j.buildenv.2011.08.014.

[11] H. Mittal, A. Sharma, and A. Gairola, “A review on the study of urban wind at the pedestrian level around buildings,” Jul. 01, 2018, Elsevier Ltd. doi: 10.1016/j.jobe.2018.03.006.

[12] S. Murakami and H. Komine, “Amplification of Wind Speed at Ground Level due to Construction of High-Rise Building In Urban Area*,” *Journal of Wind Engineering and Industrial Aerodynamics*, vol. 4, no. 3-4, pp. 343-370, 1979.

[13] X. Zhang et al., “Pedestrian wind comfort near a super-tall building with various configurations in an urban-like setting,” *Build Simul*, vol. 13, no. 6, pp. 1385–1408, Dec. 2020, doi: 10.1007/s12273-020-0658-6.

[14] Y. Du and C. M. Mak, “Improving pedestrian level low wind velocity environment in high-density cities: A general framework and case study,” *Sustain Cities Soc*, vol. 42, pp. 314–324, Oct. 2018, doi: 10.1016/j.scs.2018.08.001.

[15] Y. Tominaga et al., “AIJ guidelines for practical applications of CFD to pedestrian wind environment around buildings,” *Journal of Wind Engineering and Industrial Aerodynamics*, vol. 96, no. 10–11, pp. 1749–1761, Oct. 2008, doi: 10.1016/j.jweia.2008.02.058.

[16] J. Franke, A. Hellsten, K. H. Schlünzen, and B. Carissimo, “The COST 732 Best Practice Guideline for CFD simulation of flows in the urban environment: A summary,” *Int J Environ Pollut*, vol. 44, no. 1–4, pp. 419–427, 2011, doi: 10.1504/IJEP.2011.038443.

[17] Y. Tominaga and B. Blocken, “Wind tunnel analysis of flow and dispersion in cross-ventilated isolated buildings: Impact of opening positions,” *Journal of Wind Engineering and Industrial Aerodynamics*, vol. 155, pp. 74–88, Aug. 2016, doi: 10.1016/j.jweia.2016.05.007.

[18] J. Liu and J. Niu, “CFD simulation of the wind environment around an isolated high-rise building: An evaluation of SRANS, LES and DES models,” *Build Environ*, vol. 96, pp. 91–106, Feb. 2016, doi: 10.1016/j.buildenv.2015.11.007.

[19] R. F. Warming and R. M. Beam, “Upwind second-order difference schemes and applications in aerodynamic flows,” *AIAA Journal*, vol. 14, no. 9, pp. 1241–1249, 1976, doi: 10.2514/3.61457.

[20] A. Harten, “High Resolution Schemes for Hyperbolic Conservation Laws,” *J Computational Physics*, vol. 49, no. 3, pp. 357-393, 1983, doi:10.1016/0021-9991(83)90136-5.

[21] H. Tanaka, R. Yoshie, and C.-H. Hu, “Uncertainty in Measurements of Velocity and Concentration around a Building,” in the *4th International Symposium on Computational Wind Engineering*, 2006, pp. 549–552.